Synuclein-γ Is Closely Involved in Perineural Invasion and Distant Metastasis in Mouse Models and Is a Novel Prognostic Factor in Pancreatic Cancer

Taizo Hibi,[1,2,3] Taisuke Mori,[1] Mariko Fukuma,[1] Ken Yamazaki,[1] Akinori Hashiguchi,[1] Taketo Yamada,[1] Minoru Tanabe,[2] Koichi Aiura,[2] Takao Kawakami,[4] Atsushi Ogiwara,[5] Tomoo Kosuge,[3] Masaki Kitajima,[2] Yuko Kitagawa,[2] and Michiie Sakamoto[1]

Abstract

Purpose: Perineural invasion is associated with the high incidence of local recurrence and a dismal prognosis in pancreatic cancer. We previously reported a novel perineural invasion model and distinguished high – and low – perineural invasion groups in pancreatic cancer cell lines. This study aimed to elucidate the molecular mechanism of perineural invasion.

Experimental Design: To identify key biological markers involved in perineural invasion, differentially expressed molecules were investigated by proteomics and transcriptomics. Synuclein-γ emerged as the only up-regulated molecule in high – perineural invasion group by both analyses. The clinical significance and the biological property of synuclein-γ were examined in 62 resected cases of pancreatic cancer and mouse models.

Results: Synuclein-γ overexpression was observed in 38 (61%) cases and correlated with major invasive parameters, including perineural invasion and lymph node metastasis ($P < 0.05$). Multivariate analyses revealed synuclein-γ overexpression as the only independent predictor of diminished overall survival [hazard ratio, 3.4 (95% confidence interval, 1.51-7.51)] and the strongest negative indicator of disease-free survival [2.8 (1.26-6.02)]. In mouse perineural invasion and orthotopic transplantation models, stable synuclein-γ suppression by short hairpin RNA significantly reduced the incidence of perineural invasion ($P = 0.009$) and liver/lymph node metastasis ($P = 0.019$ and $P = 0.020$, respectively) compared with the control.

Conclusions: This is the first study to provide *in vivo* evidence that synuclein-γ is closely involved in perineural invasion/distant metastasis and is a significant prognostic factor in pancreatic cancer. Synuclein-γ may serve as a promising molecular target of early diagnosis and anticancer therapy.

Pancreatic ductal adenocarcinoma is currently the fourth leading cause of cancer-related death in Western countries (1). At the time of diagnosis, >80% of patients have locally advanced or metastatic disease and thus are not amenable for resection (2). Even in patients who underwent a histologically curative operation, long-term survival is rare, with the overall 5-year survival rates ranging from 10% to 25% (3, 4). Extensive local infiltration and early lymphatic and hematogenous spread likely contribute to the poor outcome of pancreatic cancer. Various criteria, such as tumor size, negative resection margins, histologic differentiation, lymph node metastasis, vascular involvement, and perineural invasion, have been proposed as prognostic indicators, but the results to date have been inconsistent (3–6). Of these, aggressive tumor extension into the perineural space even in the early stage of disease is a distinct mode of tumor spread in pancreatic cancer. High prevalence of local tumor recurrence even after curative resection is attributed to the residual tumor cells in the nerves of the remnant pancreas as well as the extrapancreatic nerve plexus that are undetected during the operation, leading to diminished survival. The striking incidence of perineural invasion in pancreatic cancer, ranging from 50% to 90%, underscores its importance (5, 6).

Recently, we established a mouse perineural invasion model and five human pancreatic cancer cell lines were divided into the high and the low–perineural invasion group (7). In the current study, proteomic analysis was used to compare protein expression profiles between these two groups to identify

Authors' Affiliations: Departments of [1]Pathology and [2]Surgery, Keio University School of Medicine; [3]Hepatobiliary and Pancreatic Surgery Division, National Cancer Center Hospital; [4]Clinical Proteome Center, Tokyo Medical University; and [5]Medical ProteoScope Co., Ltd., Tokyo, Japan

Received 11/11/08; revised 1/14/09; accepted 1/20/09; published OnlineFirst 4/7/09.

Grant support: The 21st Century Center of Excellence program and Cancer Research from the Ministry of Education, Science and Culture of Japan, and the 3rd Term Comprehensive 10-Year Strategy for Cancer Control from the Ministry of Health, Labor, and Welfare of Japan.

The costs of publication of this article were defrayed in part by the payment of page charges. This article must therefore be hereby marked *advertisement* in accordance with 18 U.S.C. Section 1734 solely to indicate this fact.

Note: Supplementary data for this article are available at Clinical Cancer Research Online (http://clincancerres.aacrjournals.org/).

Requests for reprints: Michiie Sakamoto, Department of Pathology, Keio University School of Medicine, 35 Shinanomachi, Shinjuku-ku, Tokyo 160-8582, Japan. Phone: 81-3-5363-3764; Fax: 81-3-3353-3290; E-mail: msakamot@sc.itc.keio.ac.jp.

doi:10.1158/1078-0432.CCR-08-2946

Translational Relevance

Aggressive tumor extension into the perineural space and adjacent lymph nodes even in the early stage of disease is a distinct mode of tumor spread in pancreatic cancer; however, its molecular mechanism remains unclear. This is the first study describing *in vivo* evidence that synuclein-γ is closely involved in perineural invasion/distant metastasis using mouse models and is a significant predictor of survival in resected cases of pancreatic cancer. Because 33% of patients with stage I disease in our series showed synuclein-γ overexpression, synuclein-γ may become an indicator for early diagnosis. To optimize the magnitude of pancreatic surgery, the extent of neural plexus resection and lymph node dissection may be determined according to the preoperative synuclein-γ status. Stratification of resected cases by synuclein-γ status is also worth considering to customize postoperative multidisciplinary approach. Synuclein-γ may well serve as a novel molecular target of anticancer therapy of this devastating disease.

differentially expressed proteins that may play a role in perineural invasion, reflecting the more aggressive tumor phenotype. Among the overexpressed proteins that emerged from quantitative proteomics, we selected synuclein-γ (SNCG) for further investigation because its corresponding mRNA was also up-regulated in the high–perineural invasion group (7). To clarify the clinical significance of SNCG expression in pancreatic cancer, the medical records of resected cases were retrospectively reviewed, focusing on the correlations with clinicopathologic factors as well as prognosis. The effect of stable SNCG suppression in the high–perineural invasion group was evaluated *in vivo* using mouse perineural invasion and orthotopic transplantation models.

Materials and Methods

Cell lines and laboratory animals. Five human pancreatic cancer cell lines, Capan-1, Capan-2, AsPC-1, Panc-1, and HPAF-II, were obtained from the American Type Culture Collection. Eight- to 12-wk-old, nonobese diabetes/severe combined immunodeficient mice were used. All studies were conducted in accordance with the U.S. Public Health Service Policy on Humane Care and Use of Laboratory Animals, NIH.

Perineural invasion model and orthotopic (pancreas) transplantation model in mice. The human pancreatic cancer cell lines were harvested from confluent cultures, washed twice with PBS, and resuspended in a serum-free RPMI 1640. For the perineural invasion model, mice were anesthetized, and 6 to 7 × 10^6 viable tumor cells in 100 μL of cell suspension were injected s.c. on the midline of their backs at two sites using an inoculator fitted with a 23-gauge needle. Six to 8 wks after injection, the tumor was resected with a 5-mm margin of the neighboring skin to examine the degree of perineural invasion to the mouse s.c. nerves (7).

For the orthotopic transplantation model, the mice were anesthetized and the distal pancreas exteriorized as described previously (8), and ~ 10^6 viable tumor cells in 10 μL of cell suspension were injected into the pancreas using an inoculator with a 27-gauge needle. The pancreas was relocated into the abdominal cavity, and the peritoneum and skin were closed with a surgical stapler. Five to 6 wks after injection, the mice were sacrificed, and the pancreas, stomach, duodenum, liver, lymph nodes, lungs, and other organs of suspected tumor involvement or metastasis were harvested.

Proteomic analysis. Tumor cells of the human pancreatic cancer cell lines were homogenized in PBS supplemented with a protease inhibitor cocktail (Roche Diagnosis) and fractionated by ultracentrifugation (52,000 × *g*; 4°C; 20 mins). The resulting pellet, containing plasma membranes from the cells, was solubilized in PBS containing 5% SDS with continuous ultrasonication. The resulting solution was taken as the insoluble fraction, whereas the supernatant from the ultracentrifugation, containing mainly cytosolic proteins, was taken as the soluble fraction. An aliquot (50 μg of protein) from each fraction was subjected to SDS-PAGE on a 12.5% polyacrylamide gel 1 mm thick. SDS-PAGE was carried out until the bromophenol blue marker passed the boundary between the stacking and separation gels so that almost all proteins were condensed in a small area between the gel boundary and the blue marker. This small gel area was then excised from the gel slab, and the gel slice, including proteins, was subjected to in-gel tryptic digestion (9).

The resulting small peptide mixture (1 μg) was analyzed using a liquid chromatography–tandem mass spectrometry (MS/MS) system in a fully automated manner (10, 11). A reversed-phase peptide separation was done on a C18 capillary column (Michrom Bioresources) at a flow rate of 1 μL/min. The liquid chromatography effluent was directly interfaced with an electrospray ionization source in a positive ion mode modified on a Finnigan LTQ linear ion trap mass spectrometer (Thermo Fisher Scientific; ref. 12). The electrospray ionization–MS/MS operation and continuous data acquisition of full MS scan and subsequent three MS/MS scans were carried out on an Xcalibur system controller (Thermo Fisher Scientific).

All full MS data were investigated using an i-OPAL differential liquid chromatography -MS data analysis system (i-OPAL algorithm; patent WO2004/090526 AI). Firstly, the signal intensity of the full MS scan was normalized so that the total signal intensity of each data became the same value. Several standard signals, derived either from the coanalyzed egg white lysozyme or from sample intrinsic common proteins, were selected as i-OPAL alignment markers. The i-OPAL alignment program was used to align the nonlinearly fluctuating liquid chromatography retention time axis of all liquid chromatography -MS data to finally generate a single combined liquid chromatography -MS data for the soluble fraction and the insoluble fraction, respectively. A *t* test was applied for each peak signal in the final combined liquid chromatography -MS data to select candidate marker signals whose intensity differed significantly within a cell type. Statistical analysis was done using Spotfire DecisionSite software package.

All MS/MS data were investigated using Mascot search program (Matrix Science;[6] ref. 13) against the *Homo sapiens* (human) subset of the Swiss-Prot and the RefSeq protein sequence databases. The database searches were done allowing for fixed modification of cysteine residue (*S*-carbamidomethylation, +57.0 Da) and variable modification of methionine residue (oxidation, +16.0 Da), peptide mass tolerance at ±2.0 Da, and product ion tolerance at ±0.8 *m/z* unit.

The proteomic analysis was done in duplicate for each cell line. An liquid chromatography -MS/MS measurement generated a single two-dimensional signal profile and >10,000 product ion spectra acquired by dissociation of peptide ions. To identify proteins involved in perineural invasion, we compared the signal profiles between the high– and low–perineural invasion cell line groups. We filtered all the peaks detected in the signal profiles according to the following conditions: (*a*) the liquid chromatography retention time between 5 and 75 mins, (*b*) the *m/z* value of ≤1,500, and (*c*) the *P* value of the Student's *t* test between the high–perineural invasion and the low–perineural invasion groups <0.001.

Patients and resected specimens. We reviewed the medical records of 67 consecutive patients who underwent resection with curative intent for invasive ductal pancreatic adenocarcinoma from 1995 through 2004 at Keio University Hospital, Tokyo, Japan. Five patients who suffered

[6] http://www.matrixscience.com

in-hospital death were excluded, and a total of 62 patients with available follow-up data comprised the subjects of this retrospective study. Two pathologists examined all resected specimens to confirm the histopathologic diagnosis of pancreatic adenocarcinoma according to the Japan Pancreas Society Classification (14). The tumor node metastasis system of the Unio Internationale Contra Cancrum (UICC) was used for staging (15). This study was conducted under the approval of the Ethics Committee of Keio University School of Medicine (approval 16-34-1).

The definition and the degree of perineural invasion were determined as described previously (7). Other pathologic factors are summarized in Table 1. Outcome measures included disease-free and overall survival. The diagnosis of tumor recurrence or metastasis was based on radiological findings. Survival time was calculated as the period from the date of surgery until death or the most recent clinic visit.

Immunologic analysis and quantitative reverse transcriptase-PCR. A goat anti-SNCG polyclonal antibody (Santa Cruz Biotechnology) was utilized. Immunohistochemical staining was evaluated by two independent observers who were not aware of the clinicopathologic data of the corresponding tumor in the surgical cases and the SNCG suppression status in the mouse models. Positive control samples were described previously (16). In the surgical specimens, peripheral nerves also served as an internal control. SNCG positive was defined as ≥10% staining of the tumor. Immunofluorescence, Western blotting, and quantitative reverse transcriptase-PCR analysis were described previously (7). In quantitative reverse transcriptase-PCR, the primer set was 5′-AACACTGTGGCCACCAAGAC-3′ (forward) and 5′-GATGGCCTCAAGTCCTCCTT-3′ (reverse), which corresponds to the coding region of the SNCG transcript.

Vector construction and retroviral infection. Vector construction and production of recombinant retroviruses were described previously (17, 18). To generate two short hairpin RNA (shRNA) expression vectors for SNCG, that is, pSI-CMSCVpuro-H1R-SNCGshRNA-A and pSI-CMSCVpuro-H1R-SNCGshRNA-B, the targeted sequences were 5′-TGGAGGAGGCGGAGAACAT-3′ and 5′-CCGAGAAGACCAAGGAGCA-3′, respectively. For the control (nontargeting sequence) shRNA expression vector, namely, pSI-CMSCVpuro-H1R-Control, the sequence was 5′-TAAGGCTATGAAGAGATAC-3′. Two stable SNCG-suppressed Capan-1 cells and the Control Capan-1 cells were designated sh-A, sh-B, and sh-Control, respectively.

Statistical analysis. Unless otherwise indicated, all data were determined from three independent experiments, with each of them done in triplicate. The data are expressed as mean values ± SD. The mRNA levels of SNCG in each cell line were compared by Student's *t* test (two tailed). The χ^2 test or Fisher's exact probability test were used when appropriate to determine the correlations between clinicopathologic variables and SNCG expression. Survival rates were calculated with the Kaplan-Meier method, and the log-rank test was applied to compare survival between different groups. Significant prognostic factors revealed by the log-rank tests were included in the multivariate analysis using the Cox proportional hazard model. Statistical significance was defined as $P < 0.05$. All statistical analyses were done using SPSS statistical software (SPSS, Inc.).

Table 1. Correlations between SNCG expression and histopathologic factors

Variables	SNCG expression, *n* (%)		*P*
	Negative, *n* = 24	Positive, *n* = 38	
Tumor size, mm			0.014
≤20	11 (46)	6 (16)	
>20	13 (54)	32 (84)	
Serosal invasion			0.081
Absent	22 (92)	28 (74)	
Present	2 (8)	10 (26)	
Retroperitoneal extension			0.84
Absent	12 (50)	18 (47)	
Present	12 (50)	20 (53)	
Portal vein involvement			0.97
Absent	14 (58)	22 (58)	
Present	10 (42)	16 (42)	
Lymph node metastasis			0.009
Negative	12 (50)	7 (18)	
Positive	12 (50)	31 (82)	
Resection status			0.15
R0	19 (79)	24 (63)	
R1	5 (21)	14 (37)	
UICC stage			0.009
IA/IB/IIA	12 (50)	7 (18)	
IIB/III/IV	12 (50)	31 (82)	
Histologic differentiation			0.069
Well	11 (46)	9 (24)	
Moderate, poor	13 (54)	29 (76)	
Lymphatic invasion			0.091
0-1	16 (67)	17 (45)	
2-3	8 (33)	21 (55)	
Vascular invasion			0.027
0-1	17 (71)	16 (42)	
2-3	7 (29)	22 (58)	
Perineural invasion			0.033
0-1	12 (50)	9 (24)	
2-3	12 (50)	29 (76)	

Results

Proteomic analysis. We obtained 214 peaks in which 171 were up-regulated and 43 were down-regulated. A two-way hierarchical clustering algorithm successfully distinguished between the high–perineural invasion and the low–perineural invasion groups (Fig. 1A). Peptide identifications to the product ion spectra were screened according to a Mascot scoring value as the ion score representing the significance of identification. The peptide identification of the highest ion score with >30 was adopted per peak. Of the 214 peaks, 211 were linked to specific peptide identification, whereas the remaining 3 peaks were given with no identification under the present conditions. Database entry names from Swiss-Prot[7] or RefSeq[8] as the source of the peptide identifications are shown in Fig. 1A.

SNCG expression in human pancreatic cancer cell lines. Among the proteins listed in Fig. 1A, SNCG was selected for further investigation because its corresponding RNA level also showed significant up-regulation in the previous microarray analysis comparing the high– and low–perineural invasion groups (7). Quantitative reverse transcriptase-PCR was used for total RNA samples isolated from five pancreatic cancer cell lines to analyze the SNCG mRNA levels. The relative expression level of SNCG was significantly higher in the high–perineural invasion group compared with the low–perineural invasion group ($P = 0.0001$; Fig. 1B). Protein overexpression of SNCG in Capan-1 and Capan-2 was subsequently confirmed by Western blotting (Fig. 1B).

The immunohistochemical properties of cell lines for SNCG were evaluated in the tumors of the mouse perineural invasion model. SNCG staining was strongly positive (>90% of all tumor

[7] http://br.expasy.org/sprot/
[8] http://www.ncbi.nlm.nih.gov/RefSeq/

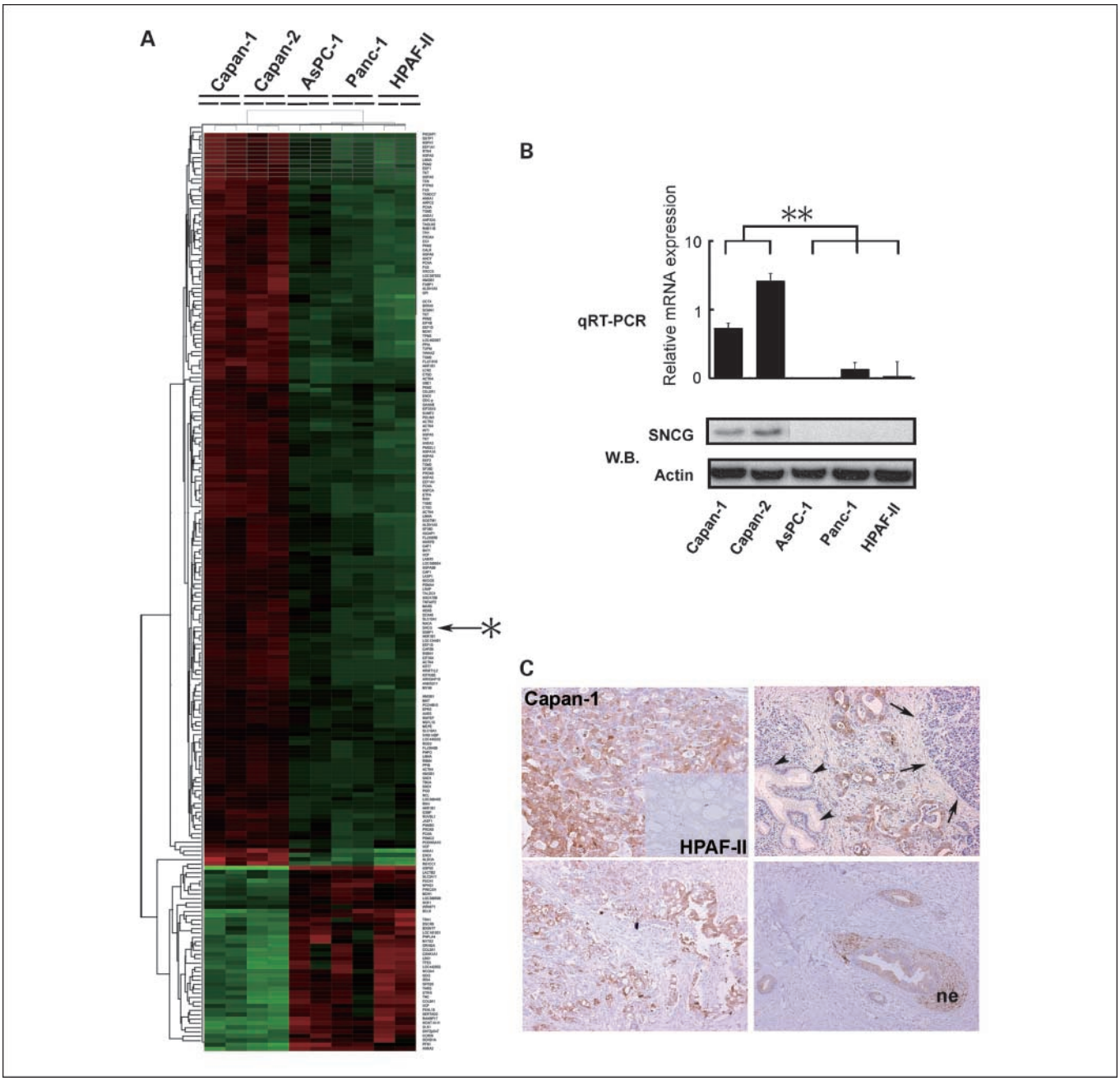

Fig. 1. *A,* proteomic analysis. Two-way hierarchical clustering algorithm successfully differentiated 214 peptide ion signals by peak intensity between high – perineural invasion (Capan-1 and Capan-2) and low – perineural invasion (AsPC-1, Panc-1, and HPAF-II) groups. Color patch, the peak intensity of the corresponding peptide in each cell line as a continuum of relative expression levels from lowest (*green*) to highest (*bright red*). *, SNCG. *B,* quantitative reverse transcriptase-PCR analysis and Western blotting. W.B., Western blotting. of SNCG in five human pancreatic cancer cell lines. SNCG mRNA and protein expression levels were significantly higher in the high – perineural invasion group compared with the low – perineural invasion group. **, $P = 0.0001$. *C, top left plate*, immunohistochemical properties of cell lines. Capan-1 showed strongly positive staining for SNCG compared with consistently negative HPAF-II (*inset*). *Top right/bottom left/bottom right plates*, in surgically resected specimens, the pancreatic cancer cells showed heterogeneous staining for SNCG, whereas the normal pancreas (*arrowheads*, pancreatic ducts; *arrows*, acinar cells) were mostly negative. ne, nerves.

cells) in the high – perineural invasion group, whereas the low – perineural invasion group was universally negative under the same condition (Fig. 1C). SNCG localization was observed mainly in the cytoplasm with focal nuclear staining.

Clinical significance of SNCG overexpression in resected cases of pancreatic cancer. The median age of the 62 patients (40 men and 22 women) meeting our eligibility criteria was 67 years (range, 45-83 years). Two tumors were categorized as UICC stage IA, 4 as stage IB, 13 as stage IIA, 34 as stage IIB, 1 as stage III, and 8 as stage IV. All stage IV cases were nodal metastasis beyond the regional lymph node station, including the para-aorta ($n = 6$), the distal mesenteric ($n = 1$), and the lesser curvature of the stomach ($n = 1$). Figure 1C exemplifies the representative SNCG staining properties of the resected specimens. The pancreatic ducts and the acinar cells of the nontumorous pancreas showed mostly negative to faint

staining. A wide range of immunoreactivity was observed in the surgical cases, varying from the cytoplasm only (focal or diffuse) to strong accumulation in the nuclei. The peripheral nerves constantly showed intense SNCG staining and therefore served as an internal positive control.

Of the total of 62 resected pancreatic cancer samples, 38 (61%) were positive and 22 (39%) were negative for SNCG staining. χ^2 analysis revealed that perineural invasion (grades 2 and 3) and other histologic markers of aggressive disease, including tumor size > 20 mm, positive lymph node metastasis, UICC stage > IIB, and vascular invasion (grades 2 and 3), were significantly associated with SNCG overexpression (Table 1).

During a median follow-up of 25 months (range, 4-171 months), the overall 5-year survival rate was 32%, with a median survival of 29 months [95% confidence interval (95% CI), 11-47 months]. Log-rank analysis showed that pancreatic cancer with SNCG overexpression had a significantly decreased overall survival, with a median of 15 months (95% CI, 9-22 months) compared with SNCG-negative tumors (median survival not reached; $P = 0.002$; Fig. 2). Positive lymph node metastasis, UICC stage $\geq$ IIB, moderately or poorly differentiated histology, and lymphatic invasion (grades 2 and 3) were also associated with a poor prognosis by univariate analysis (Table 2). Multivariate analysis based on the Cox proportional hazard model including these five factors revealed SNCG overexpression to be the only independent negative prognostic variable of overall survival (hazard ratio, 3.4; 95% CI, 1.51-7.51; $P = 0.003$). Meanwhile, patients having tumors with positive lymph node metastasis, UICC stage $\geq$ IIB, lymphatic/vascular invasion (grades 2 and 3), perineural invasion (grades 2 and 3), and SNCG overexpression were found to have significantly shorter disease-free survival (Table 2). By multivariate analysis, SNCG overexpression was the strongest negative predictor of disease-free survival (hazard ratio, 2.8; 95% CI, 1.26-6.02; $P = 0.011$), followed by positive lymph node metastasis (hazard ratio, 2.4; 95% CI, 1.03-5.57; $P = 0.044$).

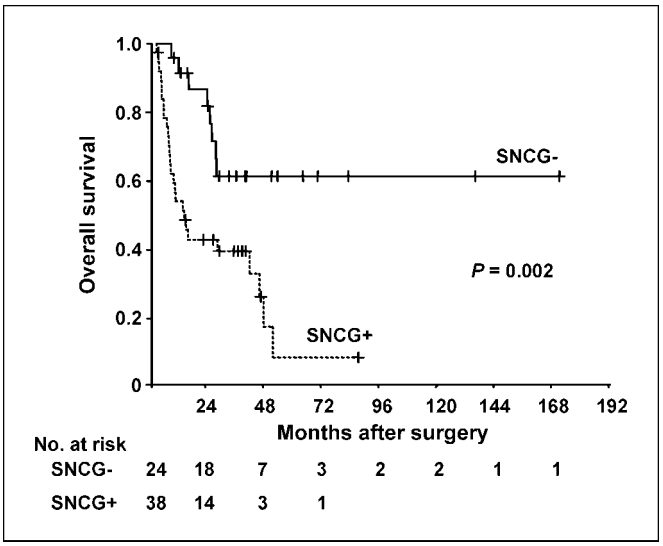

Fig. 2. Comparison of Kaplan-Meier survival curves. Patients with SNCG xoverexpression (*dotted line*) had a significantly poor prognosis compared with patients with negative SNCG expression (*solid line*).

Table 2. Log-rank univariate analysis of overall and disease-free survival

Variables	Overall survival		Disease-free survival	
	Median, mo	*P*	Median, mo	*P*
Tumor size, mm		0.059		0.060
≤20	NR		NR	
>20	25		13	
Serosal invasion		0.65		0.70
Absent	29		35	
Present	15		25	
Retroperitoneal extension		0.68		0.38
Absent	42		40	
Present	29		18	
Portal vein involvement		0.24		0.20
Absent	42		35	
Present	15		10	
Lymph node metastasis		0.016		0.006
Negative	NR		NR	
Positive	17		10	
Resection status		0.052		0.12
R0	42		35	
R1	12		8	
UICC stage		0.043		0.021
IA/IB/IIA	NR		NR	
IIB/III/IV	17		13	
Histologic differentiation		0.022		0.14
Well	NR		49	
Moderate, poor	25		18	
Lymphatic invasion		0.016		0.021
0-1	NR		40	
2-3	15		10	
Vascular invasion		0.23		0.030
0-1	42		NR	
2-3	18		13	
Perineural invasion		0.087		0.031
0-1	NR		NR	
2-3	26		12	
Intraoperative radiation		0.54		0.78
Yes	46		25	
No	28		28	
Adjuvant chemotherapy		0.14		0.98
Yes	42		18	
No	25		25	
SNCG expression		0.002		0.001
Negative	NR		NR	
Positive	15		10	

Abbreviation: NR, not reached.

***Effect of SNCG suppression* in vitro *and* in vivo.** To determine whether SNCG is an instigator of invasion and metastasis or merely a correlative product during pancreatic cancer progression, the effect of SNCG suppression on high–perineural invasion group of human pancreatic cancer cell lines was further evaluated. Capan-1 was selected for the study because the infection rate of recombinant retroviruses with shRNA for SNCG was considerably lower in Capan-2 compared with Capan-1 (data not shown). Of the two stable SNCG-suppressed Capan-1 cells, a significant decrease of SNCG mRNA and protein levels in sh-A was shown by quantitative reverse transcriptase-PCR and Western blot analysis compared with sh-Control *in vitro* ($P < 0.0001$; Fig. 3A,). In sh-B, the decline was subtle and the difference was not statistically significant ($P = 0.096$; Fig. 3A).

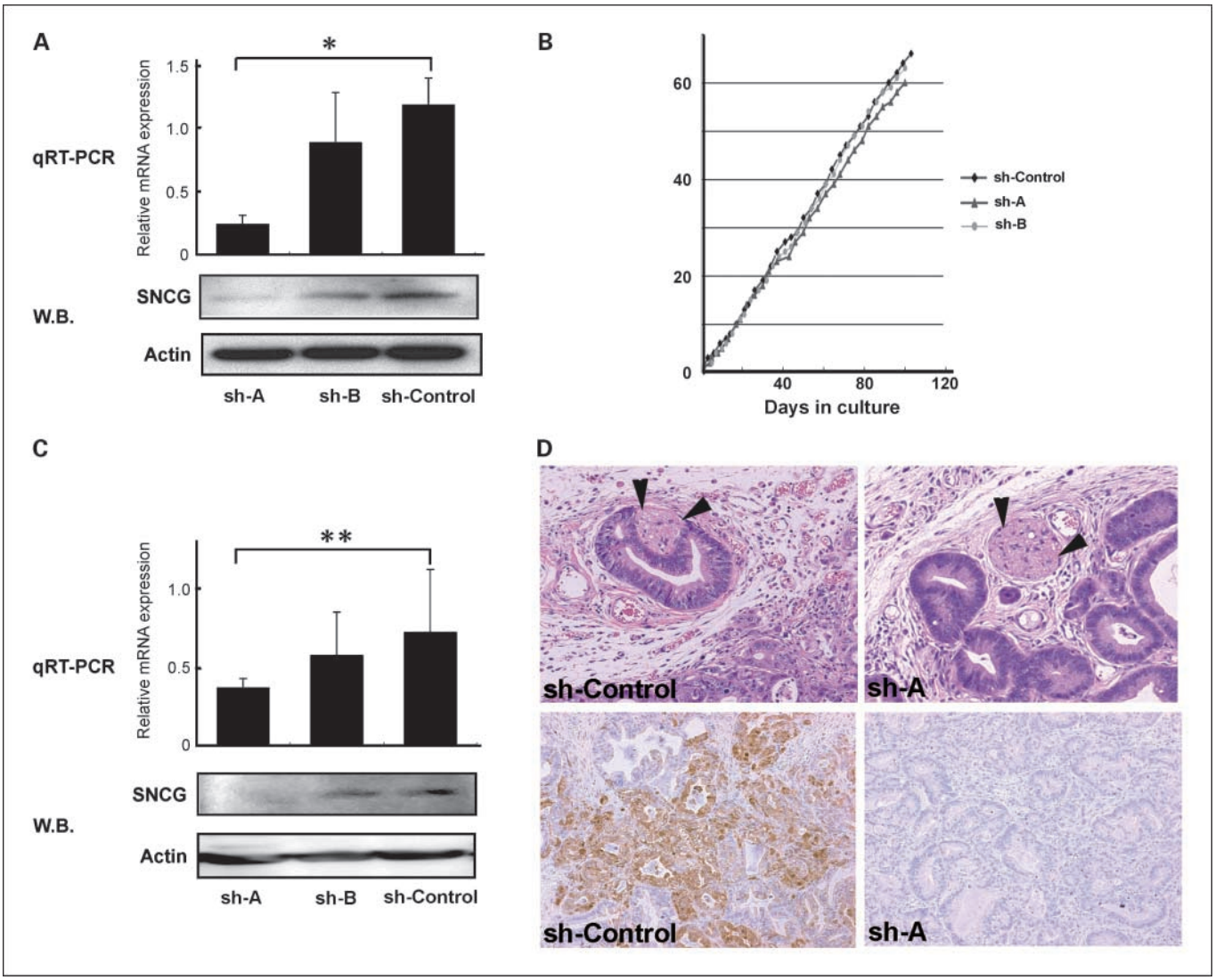

Fig. 3. *A,* quantitative reverse transcriptase-PCR analysis and Western blotting of SNCG in gene suppression study *in vitro* confirmed a substantial decrease in SNCG expression in sh-A compared with sh-Control. *, $P < 0.0001$. The difference was not statistically significant in sh-B ($P = 0.096$). *B, in vitro* growth curves of SNCG knockdown cells and control cells. The population doubling time of sh-A (*triangles*) was slightly extended compared with sh-Control (*diamonds*) and sh-B (*circles*). PD, population doubling time. *C,* quantitative reverse transcriptase-PCR and Western blotting of the s.c. tumors in mouse perineural invasion models revealed a stable *SNCG* gene knockdown effect in sh-A compared with sh-Control. **, $P = 0.018$. *D,* microscopic findings in mouse perineural invasion models. The tumor cells of sh-Control easily invaded the s.c. nerve (*arrowheads, top left plate*) and showed diffusely positive staining to SNCG (*bottom left plate*). In contrast, sh-A – derived tumors exhibited no perineural invasion, although the nerve (*arrowheads*) was involved within the tumor (i.e., nerve involvement, cancer nest includes nerves without direct contact between the tumor cells and the perineurium; *top right plate*). They were generally negative for SNCG (*bottom right plate*).

To determine whether SNCG suppression affects the *in vitro* growth of Capan-1 cells, cultures of sh-Control, sh-A, and sh-B were initially seeded at 1×10^5 cells/10-cm plate in 10 mL of RPMI 1640 serum. The population doubling time was roughly equivalent in the first 40 days in culture, although slight extension was observed in sh-A thereafter (Fig. 3B). Immunofluorescence analysis of sh-Control and sh-A under a confocal laser scanning microscope (LSM 510, Carl Zeiss) are shown in Supplementary Fig. S4A and B. In sh-Control, SNCG (*green*) diffusely localized to the cytoplasm, whereas in sh-A, the cytoplasmic SNCG signal was much lower, leaving only punctuate staining (Fig. 4A and B, respectively; Supplemental Data). No apparent difference was noted in cell shape and intercellular relations.

The results of mRNA assay and Western blotting of the s.c. tumors in the mouse perineural invasion model confirmed stable SNCG suppression in sh-A (Fig. 3C). In sh-B, the degree of down-regulation was mild, correlating with the *in vitro* results (Fig. 3A and C). In the mouse perineural invasion model, sh-A and -B showed significantly lower perineural invasion rates at 25% ($P = 0.009$) and 33% ($P = 0.026$), respectively, compared with the high perineural invasion incidence (82%) in sh-Control (Table 3). Tumor growth was also inhibited to some extent in the knockdown group, exhibiting a >25% size difference in sh-A ($P = 0.016$); however, the difference was not statistically significant in sh-B ($P = 0.27$; Table 3). A remarkable difference about the affinity of tumor cells to the mouse s.c. nerves was observed between sh-Control

and sh-A (Fig. 3D). The number of SNCG-positive cells was significantly smaller in sh-A (11% ± 11%; $P < 0.0001$) and sh-B (46% ± 12%; $P = 0.0005$) compared with sh-Control (65% ± 11%; Fig. 3D). In the invasive front of sh-Control–derived tumors, the cancer cells easily infiltrated into the muscle layers, whereas sh-A–derived tumors predominantly presented expansive growth (Supplementary Fig. S4C and D, respectively).

Because the clinicopathologic analysis of surgical cases suggest a strong correlation between SNCG overexpression and lymph node metastasis (Table 1), we constructed an orthotopic (pancreas) transplantation model to examine the SNCG knockdown effect on the metastatic potential of Capan-1 cells. In sh-A, the incidence of liver and lymph node metastasis remarkably decreased compared with sh-Control, developing in 0% (0 of 9; $P = 0.019$) and 22% (2 of 9; $P = 0.020$) of transplanted mice, respectively (Table 3). Although sh-B–derived tumors showed a mild reduction in the metastatic rate against sh-Control, the differences were not statistically significant (liver, $P = 0.28$; lymph node, $P = 0.51$). Representative microscopic findings of the liver and lymph node metastasis are shown in Supplementary Fig. S4E and F, respectively.

Discussion

This is the first study to provide *in vivo* evidence that SNCG is significantly correlated with perineural invasion as well as other major invasive parameters, including tumor size, vascular invasion, lymph node metastasis, and UICC stage, in patients with pancreatic cancer. The prognostic impact of SNCG overexpression was impressive; it was the only independent predictor of diminished overall survival and the strongest negative indicator of disease-free survival by multivariate analysis. Furthermore, SNCG gene silencing in mouse models of perineural invasion and orthotopic transplantation using human pancreatic cancer cell lines was associated with a dramatic reduction of perineural invasion as well as liver and lymph node metastasis, the main homing organs of pancreatic cancer cells. Our series shed light on the critical role of SNCG overexpression in acquiring invasive and metastatic properties.

SNCG has been shown to be involved in tumorigenesis and metastasis of a wide range of malignancies; nevertheless, only one report has documented SNCG overexpression in pancreatic cancer to date (16, 19–22). In breast cancer cell lines and mammary glands, chaperone-like activity of SNCG has been described (23, 24). SNCG may potentially exert various oncogenic roles in pancreatic cancer as a chaperone protein through stimulation of signal transduction pathways that regulate cell proliferation, invasion, and metastasis.

Zhu et al. (25) suggested that pancreatic cancer cells and nerves may interact in an autocrine/paracrine manner to provide microenvironment conducive for perineural invasion. Pancreatic cancers with overexpression of nerve growth factor in the cytoplasm of tumor cells and its high-affinity receptor, tyrosine kinase receptor A, in the perineurium of pancreatic nerves exhibited significantly higher perineural invasion rates and degree of pain. Meanwhile, in human pancreatic cancer cell lines, nerve growth factor–induced pancreatic cancer cell growth seems to be mediated by phosphorylation of tyrosine kinase receptor A and mitogen-activated protein kinase (26). Because SNCG overexpression was described to modulate mitogen-activated protein kinase pathways, leading to cell survival by inhibition of apoptotic activities (27), it may also promote nerve growth factor–tyrosine kinase receptor A signaling through its chaperone-like activity, contributing to perineural invasion in pancreatic cancer.

Previous studies have shown stage-specific SNCG up-regulation in advanced breast carcinomas and other malignancies, and our results are consistent with their observations (19–22). SNCG may be involved in pancreatic cancer progression by the induction of matrix metalloproteinases and its association in tumor cell-to-stroma interaction (28, 29). Meanwhile, SNCG was suggested to stimulate disassembly of neurofilament network and to interact with microtubule-associated proteins, thus influencing cytoskeletal integrity (30, 31). In our study, the mouse models apparently exhibited infiltrative and exaggerated growth of tumors with SNCG overexpression, although no obvious differences in cell proliferation or morphology were detected *in vitro* between cells overexpressing SNCG and knockdown cells. These findings indicate that SNCG overexpression may lead to a more malignant phenotype by altering the cell architecture, growth, and motility of pancreatic cancer cells as a chaperone protein in association with the tumor microenvironment.

Currently, proteomic analysis is emerging as a novel and powerful method of detecting proteins associated with pancreatic cancer progression (32, 33). We focused on the regulatory element of perineural invasion by comparing the proteomic profiles between high– and low–perineural invasion groups in human pancreatic cancer cell lines. Previously, proteomic

Table 3. Incidence of perineural invasion and tumor spread following s.c. injection and orthotopic transplantation of Capan-1: the impact of *SNCG* gene silencing by 2 different sequences

shRNAs	Perineural invasion model		Orthotopic transplantation model				
	Perineural invasion	Tumor size, mm	Ascites	Peritoneal dissemination	Distant metastasis		
					Liver	Lymph nodes	Lungs
sh-Control	9/11 (82%)	19 ± 5	7/7 (100%)	4/7 (57%)	4/7 (57%)	6/7 (86%)	0/7 (0%)
sh-A	3/12 (25%)*	14 ± 4†	4/9 (44%)†	1/9 (11%)	0/9 (0%)†	2/9 (22%)†	0/9 (0%)
sh-B	4/12 (33%)†	17 ± 4	7/7 (100%)	4/7 (57%)	2/7 (29%)	5/7 (71%)	0/7 (0%)

*$P < 0.01$ versus sh-Control.
†$P < 0.05$ versus sh-Control.

studies were used to differentiate protein expression profiles between pancreatic cancer tissues and normal or inflamed pancreas (32, 33), and our tumor phenotype–oriented approach may become a breakthrough to genetically tailored cancer diagnosis and therapy. In our series, 33% of patients with stage I disease showed SNCG overexpression. Several authors have detected SNCG in serum and urine samples of patients with malignant tumors (19, 20, 34) and SNCG as an indicator for early diagnosis warrants further investigation. Stratification of resected cases by SNCG status is worth considering to customize postoperative multidisciplinary approach.

In conclusion, this is the first report of *in vivo* evidence that SNCG overexpression is the key biological marker of increased malignant potential and is closely involved in perineural invasion and liver/lymph node metastasis in pancreatic cancer. In surgically resected cases, SNCG is a significant prognostic factor. SNCG may serve as a novel molecular target of early diagnosis as well as antimetastatic therapy.

Disclosure of Potential Conflicts of Interest

No potential conflicts of interest were disclosed.

Acknowledgments

We thank H. Suzuki, M. Morioka, and T. Iijima for their excellent technical support.

References

1. Jemal A, Siegel R, Ward E, Murray T, Xu J, Thun MJ. Cancer statistics, 2007. CA Cancer J Clin 2007;57:43–66.
2. Wray CJ, Ahmad SA, Matthews JB, Lowy AM. Surgery for pancreatic cancer: recent controversies and current practice. Gastroenterology 2005;128:1626–41.
3. Cleary SP, Gryfe R, Guindi M, et al. Prognostic factors in resected pancreatic adenocarcinoma: analysis of actual 5-year survivors. J Am Coll Surg 2004;198:722–31.
4. Sohn TA, Yeo CJ, Cameron JL, et al. Resected adenocarcinoma of the pancreas—616 patients: results, outcomes, and prognostic indicators. J Gastrointest Surg 2000;4:567–79.
5. Pour PM, Bell RH, Batra SK. Neural invasion in the staging of pancreatic cancer. Pancreas 2003;26:322–5.
6. Biankin AV, Morey AL, Lee CS, et al. DPC4/Smad4 expression and outcome in pancreatic ductal adenocarcinoma. J Clin Oncol 2002;20:4531–42.
7. Koide N, Yamada T, Shibata R, et al. Establishment of perineural invasion models and analysis of gene expression revealed an invariant chain (CD74) as a possible molecule involved in perineural invasion in pancreatic cancer. Clin Cancer Res 2006;12:2419–26.
8. Fu X, Guadagni F, Hoffman RM. A metastatic nude-mouse model of human pancreatic cancer constructed orthotopically with histologically intact patient specimens. Proc Natl Acad Sci U S A 1992;89:5645–9.
9. Shevchenko A, Wilm M, Vorm O, Mann M. Mass spectrometric sequencing of proteins from silver-stained polyacrylamide gels. Anal Chem 1996;68:850–8.
10. Maeda J, Hirano T, Ogiwara A, et al. Proteomic analysis of stage I primary lung adenocarcinoma aimed at individualisation of postoperative therapy. Br J Cancer 2008;98:596–603.
11. Kawakami T, Tateishi K, Yamano Y, Ishikawa T, Kuroki K, Nishimura T. Protein identification from product ion spectra of peptides validated by correlation between measured and predicted elution times in liquid chromatography/mass spectrometry. Proteomics 2005;5:856–64.
12. Schwartz JC, Senko MW, Syka JE. A two-dimensional quadrupole ion trap mass spectrometer. J Am Soc Mass Spectrom 2002;13:659–69.
13. Perkins DN, Pappin DJ, Creasy DM, Cottrell JS. Probability-based protein identification by searching sequence databases using mass spectrometry data. Electrophoresis 1999;20:3551–67.
14. Japan Pancreas Society. Classification of pancreatic carcinoma. 2nd English ed. Tokyo: Kanehara; 2003.
15. Sobin LH, Wittekind CH. TNM classification of malignant tumours. 6th ed. New York: Wiley-Liss; 2002. p. 93–6.
16. Li Z, Sclabas GM, Peng B, et al. Overexpression of synuclein-gamma in pancreatic adenocarcinoma. Cancer 2004;101:58–65.
17. Haga K, Ohno S, Yugawa T, et al. Efficient immortalization of primary human cells by $p16^{INK4a}$-specific short hairpin RNA or Bmi-1, combined with introduction of hTERT. Cancer Sci 2007;98:147–54.
18. Naviaux RK, Costanzi E, Haas M, Verma IM. The pCL vector system: rapid production of helper-free, high-titer, recombinant retroviruses. J Virol 1996;70:5701–5.
19. Liu H, Liu W, Wu Y, et al. Loss of epigenetic control of synuclein-gamma gene as a molecular indicator of metastasis in a wide range of human cancers. Cancer Res 2005;65:7635–43.
20. Jia T, Liu YE, Liu J, Shi YE. Stimulation of breast cancer invasion and metastasis by synuclein gamma. Cancer Res 1999;59:742–7.
21. Yanagawa N, Tamura G, Honda T, Endoh M, Nishizuka S, Motoyama T. Demethylation of the synuclein γ gene CpG island in primary gastric cancers and gastric cancer cell lines. Clin Cancer Res 2004;10:2447–51.
22. Wu K, Quan Z, Weng Z, et al. Expression of neuronal protein synuclein gamma gene as a novel marker for breast cancer prognosis. Breast Cancer Res Treat 2007;101:259–67.
23. Jiang Y, Liu YE, Goldberg ID, Shi YE. Gamma synuclein, a novel heat-shock protein-associated chaperone, stimulates ligand-dependant estrogen receptor alpha signaling and mammary tumorigenesis. Cancer Res 2004;64:4539–46.
24. Liu YE, Pu W, Jiang Y, Shi D, Dackour R, Shi YE. Chaperoning of estrogen receptor and induction of mammary gland proliferation by neuronal protein synuclein gamma. Oncogene 2007;26:2115–25.
25. Zhu Z, Friess H, diMola FF, et al. Nerve growth factor expression correlates with perineural invasion and pain in human pancreatic cancer. J Clin Oncol 1999;17:2419–28.
26. Zhu ZW, Friess H, Wang L, et al. Nerve growth factor exerts differential effects on the growth of human pancreatic cancer cells. Clin Cancer Res 2001;7:105–12.
27. Pan ZZ, Breuning W, Giasson BI, Lee VM, Godwin AK. Gamma-synuclein promotes cancer cell survival and inhibits stress- and chemotherapy drug-induced apoptosis by modulating MAPK pathways. J Biol Chem 2002;277:35050–60.
28. Surgucheva IG, Sivak JM, Fini ME, Palazzo RE, Surguchov AP. Effect of γ-synuclein overexpression on matrix metalloproteinases in retinoblastoma Y79 cells. Arch Biochem Biophys 2003;410:167–76.
29. Bloomston M, Zervos EE, Rosemurgy AS II. Matrix metalloproteinases and their role in pancreatic cancer: a review of preclinical studies and clinical trials. Ann Surg Oncol 2002;9:668–74.
30. Buchman VL, Adu J, Pinon LG, Ninkina NN, Davies AM. Persyn, a member of the synuclein family, influences neurofilament network integrity. Nat Neurosci 1998;1:101–3.
31. Maccioni RB, Cambiazo V. Role of microtubule-associated proteins in the control of microtubule assembly. Physiol Rev 1995;75:835–64.
32. Shen J, Person MD, Zhu J, Abbruzzese JL, Li D. Protein expression profiles in pancreatic adenocarcinoma compared with normal pancreatic tissue and tissue affected by pancreatitis as detected by two-dimensional gel electrophoresis and mass spectrometry. Cancer Res 2004;64:9018–26.
33. Bloomston M, Zhou JX, Rosemurgy AS, Frankel W, Muro-Cacho CA, Yeatman TJ. Fibrinogen γ overexpression in pancreatic cancer identified by large-scale proteomic analysis of serum samples. Cancer Res 2006;66:2592–9.
34. Iwaki H, Kageyama S, Isono T, et al. Diagnostic potential in bladder cancer of a panel of tumor markers (calreticulin, gamma-synuclein, and catechol-*o*-methyltransferase) identified by proteomic analysis. Cancer Sci 2004;95:955–61.

Clinical Cancer Research

Synuclein-γ Is Closely Involved in Perineural Invasion and Distant Metastasis in Mouse Models and Is a Novel Prognostic Factor in Pancreatic Cancer

Taizo Hibi, Taisuke Mori, Mariko Fukuma, et al.

Clin Cancer Res 2009;15:2864-2871.